The combination of the PARP inhibitor olaparib and the Wee1 inhibitor AZD1775 as a new therapeutic option for small cell lung cancer.

DOI:
10.1158/1078-0432.CCR-17-2805

Document Version
Accepted author manuscript

The combination of the PARP inhibitor olaparib and the Wee1 inhibitor AZD1775 as a new therapeutic option for small cell lung cancer

Alice Lallo[1,*], Kristopher K Frese[1,*], Christopher J Morrow[1], Robert Sloane[1], Sakshi Gulati[1], Maximillian W Schenk[1], Francesca Trapani[1], Nicole Simms[1], Melanie Galvin[1], Stewart Brown[1], Cassandra L Hodgkinson[1], Lynsey Priest[1], Adina Hughes[4], Zhongwu Lai[5], Elaine Cadogan[4], Garima Khandelwal[3], Kathryn L Simpson[1], Crispin Miller[3], Fiona Blackhall[2], Mark J O'Connor[4,#], and Caroline Dive[1,#]

[1] Clinical and Experimental Pharmacology Group, Cancer Research UK Manchester Institute, University of Manchester, Manchester, M20 4BX, UK.

[2] Institute of Cancer Sciences, University of Manchester, Manchester, United Kingdom. Christie NHS Foundation Trust, Manchester, M20 4BX, UK.

[3] RNA Biology Group, Cancer Research UK Manchester Institute, University of Manchester, Manchester, M20 4BX, UK.

[4] Oncology Innovative Medicines and Early Development Biotech Unit, AstraZeneca, Cambridge, CB2 0RE, UK.

[5] Oncology Innovative Medicines and Early Development Biotech Unit, AstraZeneca, Waltham, 02451, USA.

*These authors contributed equally to this work

Running title: PARP and Wee1 inhibition in patient-derived models of SCLC

C. Dive receives funding from the Cancer Research UK Manchester Institute core (C5759/A27412), the Cancer Research UK Manchester Centre Award (C5759/A25254), the Cancer Research UK Lung Cancer Centre of Excellence Award (C5759/A20465), and the Cancer Research UK/AstraZeneca biomarkers alliance (10001080/AgrID486.

[#] Corresponding authors: Professor Caroline Dive
Cancer Research UK Manchester Institute
Clinical and Experimental Pharmacology
Wilmslow Road, Withington
Manchester
M20 4BX
Email: caroline.dive@cruk.manchester.ac.uk
Telephone +44 (0)161 446 3036
Fax +44 (0)161 446 3019

Mark J O'Connor
DNA Damage Response Biology

Oncology Innovative Medicines and Early Clinical Development
AstraZeneca
Hodgkin Building (B900),
Chesterford Research Park
Cambridge
CB10 1XL
Email: mark.j.oconnor@astrazeneca.com

Statement of translational relevance

The clinical management of small cell lung cancer (SCLC) has remained largely unchanged for over 30 years due in part to the lack of model systems that predict clinical outcomes. SCLC prognosis remains dismal. Our recent introduction of SCLC circulating tumor cell derived explant models (CDX) that can be generated from a simple patient blood draw before treatment and again after treatment upon disease relapse offers research opportunities to test new therapies and explore predictive biomarkers. Here we report promising data in multiple CDX models that supports a combination of PARP and WEE1 inhibitors in SCLC that is superior in efficacy to standard of care chemotherapy. We also identify a 'super-responder' CDX model that provides molecular insights into strategies for patient selection for this drug combination.

Abstract

Purpose: Introduced in 1987, platinum-based chemotherapy remains standard of care for small cell lung cancer, a most aggressive, recalcitrant tumor. Prominent barriers to progress are paucity of tumor tissue to identify drug targets and patient relevant models to interrogate novel therapies. Following our development of circulating tumour cell patient-derived explants (CDX) as models that faithfully mirror patient disease, here we exploit CDX to examine new therapeutic options for small cell lung cancer.

Experimental Design: We investigated the efficacy of the PARP inhibitor olaparib alone or in combination with the Wee1 kinase inhibitor AZD1775 in ten phenotypically distinct SCLC CDX *in vivo* and/or *ex vivo*. These CDX represent chemosensitive and chemorefractory disease including the first reported paired CDX generated longitudinally before treatment and upon disease progression.

Results: There was a heterogeneous depth and duration of response to olaparib/AZD1775 which diminished when tested at disease progression. However, efficacy of this combination consistently exceeded that of cisplatin/etoposide with cures in one CDX model. Genomic and protein analyses revealed defects in homologous recombination repair and oncogenes that induce replication stress (such as MYC family members), predisposed CDX to combined olaparib/AZD1775 sensitivity though universal predictors of response were not noted.

Conclusions: These preclinical data provide a strong rationale to trial this combination in the clinic informed by prevalent, readily accessed circulating tumor cell based biomarkers. New therapies will be evaluated in SCLC patients after first line chemotherapy and our data suggest that the combination of olaparib/AZD1775 should be used as early as possible and prior to disease relapse.

Introduction

Small cell lung cancer (SCLC) is an aggressive and recalcitrant neuroendocrine tumor which metastasizes early (1). The 5 year survival rate for SCLC has been less than 5% for over 30 years, despite multiple phase I clinical trials with a variety of molecularly targeted agents. While platinum-based therapies yield objective response rates in the majority of patients, this benefit is usually transient with relapse frequently occurring in less than one year from initial diagnosis (2). Recent large scale genome sequencing efforts have failed to identify recurrent actionable mutations in SCLC and the failure to improve survival rates has largely been attributed to the fact that few patients undergo surgery, and thus the amount of tissue available for research is limited and tumor biopsies at disease relapse after chemotherapy are rarely obtained (1).

We recently reported the generation of CTC-derived explant (CDX) models in which circulating tumor cells from extensive stage SCLC patients are grown subcutaneously in immunocompromised mice (3). CDX models provide additional material to examine the biology of SCLC and serve as a robust and relevant preclinical pharmacology platform to examine the efficacy of new potential therapies. Importantly, the *in vivo* response to standard of care chemotherapy in CDX models closely resembles that of the corresponding donor patient, suggesting that preclinical results for experimental therapies may be more robust for translation to the clinic than conventional cell line-based xenografts.

Proteomic profiling in lung cancer cell lines revealed elevated levels of poly (ADP-ribose) polymerase (PARP) specifically in SCLC (4). PARP is recruited to DNA single strand breaks (SSBs) where it PARylates multiple substrates including histones to facilitate the relaxation of chromatin, as well as itself. The auto-modification of PARP is required for its dissociation from DNA and subsequent repair. The mechanism of action for PARP inhibitors with single agent activity has been proposed to involve the trapping of PARP onto the DNA single-strand breaks preventing their repair and generating a potential block for cellular DNA replication (5,6). An important consequence of this and the proposed basis of monotherapy activity is the generation of DNA double strand breaks (DSBs) that would normally be repaired by the Homologous Recombination Repair (HRR) pathway. In cancers with HRR deficiency, PARP trapping will result in significant genomic instability until it is no longer sustainable and tumor cell death results (7). Although deficiencies in the breast and ovarian cancer associated genes *BRCA1* and *BRCA2* are the most investigated examples of defective components of HRR that lead to increased PARP inhibitor activity, mutations in other HRR pathways genes, including *ATM*, *ATR*, and *PALB2*, can also convey sensitivity to PARP inhibitors (8).

Wee1 is a kinase that regulates both S-phase and G2/M progression by phosphorylating and inhibiting the cell cycle dependent kinases CDK2 and CDK1 respectively. Wee1 control of CDK2 activity in S-phase is an important component of the replication stress response, whereas the control of CDK1 and the G2/M checkpoint is critical for ensuring proper DNA repair before initiating cell division (9). Initially, it was hypothesized that cells deficient for the tumor suppressor p53 were hyper-reliant on Wee1 function and the G2/M checkpoint, and that efficacy of the Wee1 inhibitors could be linked to *TP53* status (10). Subsequent experiments revealed that this correlation was not universally true, although Wee1 inhibitor activity is still likely linked to G1/S checkpoint deficiencies in one form or another (11). Recent reports suggest that cells overexpressing potent oncogenes, such as *MYC* or *CCNE1*, that induce replication stress are also more sensitive to Wee1 inhibition, but again does not appear to be a universal pre-requisite for response (9).

Given the potential for PARP inhibitors to induce S-phase damage and a subsequent dependency on Wee1 S-phase and G2/M checkpoint activities, coupled with the high mutagenic burden and proliferative rate of SCLC, we examined the efficacy of the PARP inhibitor olaparib and the Wee1 inhibitor AZD1775 in our SCLC CDX models. The most important advantage of the CDX approach is the ability to assess biology and therapy responses not only in patient derived models generated at baseline prior to any treatment, but also in CDX derived from the same patient at disease progression after treatment. Here, we examine the novel combination of olaparib and AZD1775 for the first time in 'paired' CDX, providing a clinically relevant test-bed for the introduction of new therapeutic options following first line chemotherapy.

Our studies reveal that SCLC CDX tumors exhibit a range of sensitivities to drugs targeting PARP and Wee1 as single agents, but with clear indications of enhanced efficacy when given in combination. Moreover, these studies have revealed the presence of previously unappreciated DNA damage response deficiencies in a subset of SCLC tumors. These results therefore provide a strong rationale for the clinical development of AZD1775 in combination with olaparib or other DNA damaging agents, as well as candidate biomarkers to explore in tandem towards a precision medicine approach for this disease.

Materials and methods

Study design

The primary goal of this study was to assess the efficacy of olaparib and AZD1775 montherapies, as well as the combination, in mouse models of SCLC. Sample sizes (n = 7-11 mice per cohort) was determined to detect statistically a two-fold difference in tumor response between the various treatments. Once tumours reached enrollment size, animals were allocated to different cohorts via stratified randomization in which attempts were made to evenly distribute initial tumour volume sizes. Data collection was stopped at ethical endpoints, including deterioration in health or when tumors reached ≥ four times the initial tumor volume at enrollment. If animals became ill within 3 days of enrollment, they were excluded from the experiment, regardless of which treatment they received. No other data were excluded.

CDX establishment

CDX models were generated as previously described (3). Briefly, 10ml of peripheral blood was collected from SCLC patients into EDTA tubes in accordance with the ethically approved CHEMORES protocol (07/H1014/96), processed via RosetteSep CTC Enrichment Cocktail (15167, Stemcell Technologies), and resuspended in 100µl of a 1:1 solution of HITES medium and Matrigel (354234, BD Biosciences). Cells were then subcutaneously implanted into flanks of 8-16 week old female NOD.Cg-*Prkdc*^{scid}*Il2rg*^{tm1Wjl}/SzJ (NSG) mice (Charles River). All procedures were carried out in accordance with Home Office Regulations (UK) and the UK Coordinating Committee on Cancer Research guidelines and by approved protocols (Home Office Project license nos. 40-3306/70-8252 and Cancer Research UK Manchester Institute Animal Welfare and Ethical Review Advisory Board). In a parallel patient blood sample, CTC burden was quantified via CellSearch according to manufacturer's instructions.

In vivo pharmacology studies

Therapeutic studies were carried out essentially as previously described (3). 100,000 viable CDX cells in 100µl 1:1 RPMI:matrigel were injected subcutaneously into the right flank of procedure/treatment naïve, 8-10 week old (20-25g) female C.B-17/IcrHsd-*Prkdc*^{scid}*Lyst*$^{bg-J}$ mice (Envigo). When tumors reached 150–250 mm^3, they were allocated via stratified randomisation into cohorts to be treated each morning with vehicle(s), olaparib (50 mg kg^{-1} unless indicated otherwise), AZD1775 (120 mg kg^{-1}), the combination, or topotecan using tolerated dosing regimens previously shown to optimally achieve target inhibition. Olaparib (AstraZeneca) was formulated at 10 mg ml^{-1} in 10% DMSO/30% KLEPTOSE® HPβCD and AZD1775 (AstraZeneca) was formulated at 12 mg ml^{-1} in 0.5% methylcellulose. Compounds were orally dosed at 5 ml kg^{-1} daily (olaparib) or 10 ml kg^{-1} on a 5-on, 2-

off (AZD1775) schedule for 21 days. On days when both drugs were administered, olaparib was administered 1 hour after AZD1775. Topotecan (The Christie NHS Foundation Trust) was administered at 3 mg kg^{-1} daily for three days via intraperitoneal injection. Cisplatin and etoposide (The Christie NHS Foundation Trust) were administered as previously described (3), and these studies were performed separately from studies on olaparib and AZD1775. Mice were observed for a period of time post dose to ensure no adverse effects were seen. Tumors were measured twice a week by caliper until they reached four times initial tumor volume (4×ITV), as determined by the formula $V=(L \times W^2)/2$, or until animal health deteriorated. For pharmacokinetic and pharmacodynamic studies, mice were sacrificed two or 24 hours after a single dose of indicated drugs were administered and relevant tissues were collected. Statistical assessment of tumor response was performed as described (12). Tumor growth delay (TGD) measures the normalized time to quadrupling of initial tumor growth, and therefore a higher TGD value is indicative of more robust tumor growth inhibition.

Pharmacokinetic analysis

25µl plasma was prepared using an appropriate dilution factor, and compared against an 11 point standard calibration curve (1-10,000 nM) prepared in DMSO and spiked into blank plasma. 100µl acetonitrile was added with the internal standard, followed by centrifugation, and supernatants were then diluted 1:7 in water and analysed via UPLC-MS/MS using a Xevo TQ-S mass spectrometer (Waters) and the system and optimization parameters listed (Supplementary **Table 1**, **2**) .

Ex vivo studies

CDX tumors were dissociated as previously described (13) and cells were grown in HITES medium supplemented with 5 µM Y-27632 (Selleckchem) and 2.5% FBS. CDX-derived cells were seeded into 96 well plates, incubated for 48 hours, and treated with increasing concentrations of the compound(s) of interest. Seven days after treatment, cell viability was assessed via Cell-Titer Glo 3D assay (Promega). Single dose response curves were computed with the open source CRUK software Combenefit (14). Combinatorial activity was assessed using the Loewe additivity model (15) and computed using the R package synergyfinder (16). For radiosensitization assays, cells were irradiated with indicated doses using a Gulmay Bipolar 320kV X-ray source. After irradiation cells were plated into fresh media and viability was measured after five days.

Rad51 focus assay

CDX-derived cells were irradiated with 10Gy and incubated for the indicated times. After incubation, cells were cytospun at a concentration of 150,000 cells per slides , fixed in 4% PFA for 20 min at room temperature, permeabilized with 0.2% triton X-100 (Sigma), and washed with 10% FBS 0.2%

Tween20 in PBS. Samples were then blocked with avidin/biotin blocking solution (VECTOR laboratories, SP-2001) and 10% goat serum (Dako). Sections were then incubated with primary antibodies (**Supplementary Table 3**) overnight at 4^{o}C overnight, washed, and incubated with secondary antibodies for 1 hour at room temperature. Slides were mounted in ProLong DAPI (Life Technologies) and left dry in the dark. Images were acquired with a Leica gated Stimulated Emission Depletion microscope and cells were scored as HR-proficient if there were ≥5 foci per nucleus.

Immunohistochemistry

4µm formalin fixed paraffin embedded tumor sections were stained for the indicated antigens using the BondMax autostainer and Bond polymer refine detection system (Leica Biosystems), Venatana Discovery Ultra, or I6000 BioGenex autostainer and Dako EnVision system HRP (Dako) (**Supplementary Table 3**). For these antigens, digital images of whole tissue sections were acquired using a Leica SCN400 histology scanner (Leica Microsystems). Images were analysed using Definiens Developer XD and the Tissue Studio Portal version 4.4 (Definiens AG).

Immunoblot analyses

Flash frozen CDX tumors were homogenized in Fastprep tubes with matrix A using a TissueLyser LT (Qiagen) in ice cold lysis buffer (10mM HEPES pH 7.1, 50mM NaCl, 0.3M sucrose, 0.1mM EDTA, 0.5% Triton X-100, 1mM DTT; or 20mM Tris, 137mM NaCl, 10% Glycerol, 50mM sodium fluoride, 1mM activated sodium orthovanadate , 1% SDS, 1% NP40 substitute) in the presence of Protease Inhibitor Cocktail and Phosphatase Inhibitor Cocktail I and III (Sigma-Aldrich). Protein concentration was determined by BCA protein assay reagent kit (Thermo Scientific). Protein extracts were resuspended in NuPAGE LDS sample buffer 4x (Invitrogen) and 10x NuPAGE sample reducing agent (Invitrogen). Total protein was resolved on a NuPAGE 4-12% Bis-Tris 1.0 mm gel (Invitrogen). After transfer onto PVDF or nitrocellulose membranes, blots were incubated with the appropriate primary antibody (**Supplementary Table 3**) and the corresponding horseradish peroxidase-coupled secondary IgG. Detection was obtained with the Supersignal West Dura extended duration substrate (ThermoFisher) on a ChemiGenius Imaging System (Syngene) or film.

PAR ELISA

Flash frozen CDX tumor tissue was homogenized for 3x30 seconds at speed 6.0 in Fastprep tubes with matrix A using ice cold lysis buffer (20mM Tris, 137mM NaCl, 10% Glycerol, 50mM sodium, 1mM activated sodium orthovanadate, 1% SDS, 1% NP40 substitute in the presence of protease inhibitor cocktail (Roche) and phosphatase inhibitor cocktails 2 & 3 (Sigma-Aldrich). Lysates were sonicated, incubated on ice for 30 minutes, centrifuged, and supernatants were boiled for five minutes. They were then cooled on ice for one minute, centrifuged, and protein concentration was

estimated using a Pierce BCA assay. 2µg lysate was used to quantify total PAR levels according to manufacturer's recommendations (Trevigen). Samples were quantified on a Tecan Safire II microplate reader (Tecan) and absolute values were determined via interpolation from a standard curve.

RNAseq

Total RNA was extracted from three independent RNAlater (Qiagen) -treated tumors from each model with RNeasy mini kits (Qiagen) and quantified by Qubit (Thermo Fisher). RNA with an RNA integrity number (RIN) > 8 (Agilent 2100 Bioanalyzer) was used to generate libraries with SureSelect poly A samples (Agilent) and sequenced on the NextSeq 500 using 75 bp paired end reads. RNASeq data was aligned to Human GRCh38 and Mouse GRCm38 assembly using Mapsplice (version 2.1.6). Xenograft data was filtered via a novel algorithm to distinguish human and mouse reads (17). The filtered reads are then used to generate counts data using Rsubread package (version 1.16.1) with Ensembl 77 GTF file in R. The counts were converted into RPKM values using edgeR (version 3.10.5).

Whole exome sequencing (WES)

Genomic DNA was extracted from a representative flash frozen CDX tumor from each model with DNeasy Blood and Tissue kits (Qiagen) and quantified by Qubit. 150 base pair paired-end reads were obtained from samples assessed on a NextSeq 500 High run (Illumina). The WES data was aligned to Human GRCh37 and Mouse GRCm37 assembly with bwa-mem (version 0.7.12). Deduplication, realignment and recalibration were performed on the aligned data using Picard (version 1.96) and GATK tools (version 3.3), as stated in the GATK best practices. The reads aligning to mouse genome were removed using an in-house developed algorithm (17). Somatic mutation calling was done on the filtered reads using Mutect (version 1.1.7) and the mutation calls were annotated using Ensembl Variant Effect Predictor.

Statistics

All statistical analyses were performed on Prism v7.04 (GraphPad) using one-way ANOVA or Student's t-test for multiple or single pairwise comparisons, respectively. Single and double asterisks denote $p < 0.05$ and $p < 0.005$, respectively. The absence of an asterisk means that there is no statistically significant difference between groups.

Results

To examine the efficacy of olaparib and AZD1775 in SCLC, we first treated two previously characterised CDX models representative of chemosensitive and chemorefractory patient donors (3). The chemosensitive CDX3 and chemoresistant CDX4 models were generated from baseline blood samples taken from a patient that lived for 9.7 months and 0.9 months, respectively, following treatment with platinum-based therapies. Treatment of mice bearing CDX3 tumors with either olaparib or AZD1775 monotherapy led to complete or modest regression, with tumors rapidly recurring after treatments ended (**Fig. 1, Supplementary Fig. 1a**). Remarkably, combination therapy in CDX3 promoted complete and durable regressions with 5/7 mice remaining tumor-free for over 1 year. Conversely, CDX4, a model completely resistant to cisplatin/etoposide, showed no response to olaparib whereas treatment with either AZD1775 monotherapy or the combination led to disease stabilization during the treatment period (**Fig. 1, Supplementary Fig. 1b**).

Topotecan, a DNA damaging agent that is the only approved second-line therapy for SCLC, was more effective than cisplatin/etoposide against CDX4, eliciting a median 66% tumor regression (**Supplementary Fig. 1e**). Furthermore combination of topotecan with AZD1775 yielded impressive tumor regression in this model, with median 83% tumor regression. These data indicate that AZD1775 can cooperate with an effective DNA damaging agent even in a platinum-resistant model.

The majority of SCLC patients present with chemosensitive disease followed by rapid acquisition of chemoresistance and disease progression. To examine the efficacy of the olaparib/AZD1775 combination in patients with acquired chemoresistance, we utilised a pair of CDX models, CDX8 and CDX8p, which were derived from blood samples from the same patient taken at baseline and upon disease progression after platinum treatment (**Supplementary Fig. 2a**). Treatment of CDX8 tumors with cisplatin/etoposide induced a partial response (median 47% regression) and rapid relapse (median tumor growth delay (TGD)=1.9), whereas mice bearing CDX8p received little benefit from cisplatin/etoposide treatment (median 15% growth and TGD=1.3), consistent with the outcome of chemotherapy in the donor patient (**Fig. 1, Supplementary Fig. 2b, c**). When these models were treated with olaparib or AZD1775, CDX8 exhibited relatively stable disease during the treatment period, whereas CDX8p tumors grew at the same rate as the vehicle control cohort (**Fig. 1, Supplementary Fig. 1c**, **d**). Similar to that seen in CDX3, the combination exhibited synergistic activity against CDX8 with many complete regressions. Although CDX8 tumors recurred more quickly than CDX3 tumors (**Fig. 1b**), olaparib/AZD1775 yielded a more durable response than cisplatin/etoposide (median TGD=1.9) (**Fig. 1**). Consistent with reports of reduced olaparib efficacy

against platinum-resistant ovarian cancer (18), treatment with olaparib alone or in combination with AZD1775 achieved only tumor growth delay rather than regression in CDX8p (**Fig. 1, Supplementary Fig. 1d**). Taken together these results indicate that although the efficacy of olaparib/AZD1775 was model dependent, the activity of the combination is consistently superior to that achieved with conventional cisplatin and etoposide in chemosensitive models. Furthermore, the combination of AZD1775 and an active DNA damaging agent has activity in a chemoresistant model.

As platinum-based regimens are initially quite effective in treating SCLC, it is unlikely that olaparib/AZD1775 or any other new agent will be used clinically in treatment-naïve patients. We therefore sought to examine the efficacy of olaparib/AZD1775 in a second-line setting following initial treatment with cisplatin/etoposide. Toward this end, we treated mice bearing CDX3 tumors with a single cycle of cisplatin/etoposide to induce an initial tumor response. After a three week drug holiday during which tumors began to re-grow, mice were randomized to receive vehicle, olaparib, AZD1775, or the combination. In this setting, only 1/12 combination-treated mice remained tumor free and the median time to initial tumor volume was 101 days following completion of dosing (**Supplementary Fig. 3**), suggesting that this combination is still active after initial treatment with cisplatin/etoposide but may prove most beneficial as a first-line option if the proper patient cohort could be identified.

In vivo pharmacology experiments are both time consuming and expensive, so we sought to use an *in vitro* platform to expedite drug screening as previously reported for colorectal and breast cancers (19,20). Using an *ex vivo* SCLC CDX culture system that faithfully recapitulates *in vivo* drug response in CDX models (21), we investigated the *in vitro* efficacy of olaparib, AZD1775, and the combination. Both monotherapies as well as the combination correlated with *in vivo* response, with evidence of synergy in CDX3 and CDX8, but not CDX4 or CDX8p (**Fig. 2a-d, Supplementary Fig. 4**). We therefore decided to screen additional CDX models with varying sensitivity to platinum, derived from baseline and relapse patients (**Table 1**). Examination of *ex vivo* cultures derived from CDX2, CDX3p, CDX10, CDX14p, CDX15p, and CDX15p2 revealed a range of sensitivity to cisplatin and olaparib monotherapies, whereas most models were relatively sensitive to AZD1775 with submicromolar GI_{50}'s. Similarly, the majority of models were sensitive to olaparib/AZD1775, although CDX4 and CDX8p were among the most resistant *in vitro* (**Fig. 2e**). These results from a broader panel of CDX models tested *in vitro*, support our findings that olaparib/AZD1775 is an effective combination and may represent a promising treatment for SCLC.

It has previously been reported that olaparib is a CYP3A substrate and that AZD1775 is a CYP3A4 inhibitor (22), therefore it was possible that the combination effect seen in some CDX models could

be attributed to a drug-drug interaction in which elevated levels of olaparib result from inhibition of CYP3A by AZD1775. To examine this possibility we administered 50 mg kg^{-1} olaparib (olaparib low) both alone and in combination with AZD1775 as previously described, or 100 mg kg^{-1} olaparib alone (olaparib high) to CDX3-bearing mice. Increasing the dose of olaparib to 100 mg kg^{-1} had no significant effect on anti-tumor efficacy against CDX3 (**Fig. 3a**), and pharmacokinetic analysis of olaparib and AZD1775 indicates that mice dosed with the combination are not exposed to plasma drug concentrations significantly different to mice receiving monotherapies (**Fig. 3b, c**). Therefore the efficacy of the olaparib/AZD1775 combination is unlikely to be due to altered olaparib exposure.

To examine the molecular mechanism of olaparib and AZD1775 efficacy, we treated parallel cohorts of mice with a single dose of drug and examined intra-tumor signal transduction pathways and cellular behaviour. Wee1 kinase regulates G2/M progression by directly phosphorylating and inhibiting the cell cycle kinase CDK1 and this has been used both preclinically and clinically as a pharmacodynamic biomarker of Wee1 inhibition (9). Consistent with Wee1 inhibition, phospho-CDK1 levels were reduced and the number of mitotic cells was increased in cohorts treated with AZD1775 either alone or in combination with olaparib (**Fig. 4a, c; Supplementary Fig. 5**). Similarly, global PAR levels were decreased in all cohorts treated with olaparib (**Fig. 4b**). Together these data indicate that the different levels of efficacy in different CDX models cannot be attributed to differential target inhibition. Examination of cleaved caspase 3 levels revealed that increased levels of apoptosis correlated with anti-tumor efficacy (**Fig. 4d; Supplementary Fig. 5**). Since treatment with both olaparib and AZD1775 promoted increased DNA damage, we investigated several pathways associated with the DNA damage response.

CHK1 phosphorylation by ATR is induced by the formation of regions of single strand DNA (ssDNA) either resulting from the processing of DNA double strand breaks (DSBs) or stalled DNA polymerase during DNA synthesis due to replicative stress (9). The extended ssDNA is coated by replication protein A (RPA) which binds ATR and associated proteins that initiate the replication stress response that includes the phosphorylation and activation of CHK1. The inability to resolve replication stress-induced fork stalling can lead to replication fork collapse, the generation of a single-ended DSBs, and ATM-induced H2AX phosphorylation. Consistent with previous reports, treatment with AZD1775 promoted potent CHK1 phosphorylation, indicative of Wee1 inhibition increasing replication stress (23). However, this effect was similar in all models examined and did not correlate with efficacy (**Fig. 4e, Supplementary Fig. 1**). Conversely, induction of γH2AX more closely correlated with *in vivo* efficacy and highest levels were seen when AZD1775 was combined with olaparib in CDX3 and CDX8, the two most sensitive models (**Fig. 4f, Supplementary Fig. 1**).

The *BRCA1* and *BRCA2* gene products are key DDR proteins that play different but pivotal roles in DNA DSB repair (DSBR). Both proteins have been shown to play key roles in the replication stress response as well through replication fork stabilisation and restart, and deficiencies in either lead to PARP inhibitor sensitivity (24). Given this association, we were interested to know the DSBR status in our CDX models. BRCA and broader HRR deficiencies have been identified via a variety of mechanisms including transcriptional or mutational impairment of genes that regulate homologous recombination repair, the accumulation of 'genomic scars', or functional assays such as DNA damage-induced Rad51 focus formation (24). Analysis of RNAseq data on CDX models did not reveal an obvious HRR mutation signature that correlated with sensitivity, nor did whole exome sequencing reveal an elevated mutation burden associated with impaired DSBR (**Supplementary Fig. 6a, b**). Despite the absence of an HRR mutation signature, CDX3 is exquisitely radiosensitive compared to CDX4, indicating that CDX3 is potentially deficient in DSBR (**Fig. 5a**). Functional assessment of HRR status via examination of ionizing radiation-induced Rad51 focus formation revealed that CDX3 displayed signs of HRR deficiency, suggesting this model may harbour a mutation in a gene that mediates HRR (**Fig. 5b**). PALB2 is a BRCA2-associated DDR protein required for effective HRR (9). Whole exome sequencing of CDX3 revealed a somatic mutation in *PALB2* that resulted in a stop-gain at E178 leading to premature truncation of the protein (**Fig. 5c, d**). Analysis of RNAseq data indicates that all *PALB2* reads harbour this mutation, suggesting a complete loss of the wild type allele (**Supplementary Fig. 6c**). Therefore it is highly likely that the exquisite sensitivity of CDX3 to both platinum and olaparib can be attributed to the *PALB2* mutation.

Several additional mechanisms of acquired resistance to olaparib have been reported, including activation of PI3K or Met signalling (25,26), decreased expression of *PARP1* or *SLFN11* (27-30), and restoration of DNA end resection (31). We did not find any consistent differences in MET or PI3K signaling, suggesting that activation of these kinases is not a recurrent mechanism of olaparib resistance in SCLC (**Supplementary Fig. 7a**). PARP-trapping is now recognized as the primary mechanism of PARP inhibitor-mediated cytotoxicity, and loss of expression of PARP1 is thus associated with resistance. However, expression analysis did not reveal any alteration in PARP1 expression in either CDX4 or CDX8p (**Supplementary Fig. 7b**). SLFN11 binds to RPA, and it has been postulated that high SLFN11 levels inhibit homologous recombination repair by promoting the destabilization of the interaction between RPA and ssDNA (32). Although CDX4, the most olaparib-resistant model, exhibits the lowest SLFN11 levels, this correlation does not extend to CDX8p (**Supplementary Fig. 7c**). End resection is the process of creating stretches of ssDNA necessary for Rad51-induced strand invasion and subsequent repair via homologous recombination. In the context of functionally relevant *BRCA1* mutations, decreased expression of the non-homologous end joining

(NHEJ) proteins 53BP1 and Rev7 have been reported to result in restoration of end resection activation of HRR and consequently resistance to PARP inhibitors (33,34). However, neither CDX4 nor CDX8p have decreased expression of either protein compared to CDX3 or CDX8 (**Supplementary Fig. 7c**). Although CDX8 harbours a C342F mutation in *FANCD2*, a key player in the Fanconi anaemia pathway that includes BRCA, this mutation is still present in CDX8p and, in the absence of any *TP53BP1*-associated mutation, is unlikely to explain the acquired chemoresistance manifest in CDX8p. Neither whole exome sequencing nor RNAseq has identified likely candidates of resistance, and we are actively pursuing additional strategies to discover the mechanism of acquired drug resistance in CDX8p.

One proposed predictive biomarker of AZD1775 sensitivity is the absence of a G1/S checkpoint (35). It has been hypothesized that cells with a compromised G1/S checkpoint are more dependent on the G2/M checkpoint, and therefore sensitive to Wee1 inhibition. Given the role for p53 in regulating the G1/S checkpoint, multiple studies have investigated whether p53 mutations are stand-alone biomarkers for AZD1775 sensitivity (10,36). Although all SCLC models tested harbour deleterious mutations in *TP53*, chemoresistant models tend to retain relatively high levels of the cyclin dependent kinase inhibitor $p21^{CIP1}$, a primary mediator of p53-dependent cell cycle arrest (**Fig. 6a**, **b**). Although treatment does not induce expression of $p21^{CIP1}$ (**Supplementary Fig. 8**), p53-independent activation of $p21^{CIP1}$ may partially mediate resistance to AZD1775 by maintaining the G1/S checkpoint in p53-deficient cells. The majority of SCLC cells also possess mutations in *RB1*, which regulates entry into S-phase. We therefore investigated whether *RB1* status correlates with AZD1775 sensitivity. Whole exome sequencing and RNAseq revealed RB1 mutations in CDX3 (splice mutation at 5' of exon 17, c.1499-1G>T), CDX4 (87bp deletion in exon 1 and intron 1, c.99_137+48del), and CDX8/8p (G509*), and none of the models used in this study express pRB as determined by western blotting (**Fig. 6a**). Moreover, there is no consistent correlation between cyclin/CDK expression and sensitivity to AZD1775. This does not rule out the potential importance of deregulation of the G1/S checkpoint but does suggest that, at least in SCLC, regulators of G1/S CDKs alone do not appear to be predictive biomarkers of AZD1775 sensitivity.

Low expression of PKMYT1, a cell cycle kinase that is functionally redundant to Wee1, can predispose cancer cells to AZD1775 sensitivity by lowering the threshold of kinase inhibition (37). However, while the most sensitive models do have the lowest levels of PKMYT1 RNA, there is no correlation between PKMYT1 levels and CDK1 phosphorylation, suggesting this is unlikely to be a major factor governing AZD1775 sensitivity (**Fig. 4a, Supplementary Fig. 9a**).

Several studies have reported a link between sensitivity to Wee1 inhibition and replication stress (38). Replication stress is a general term used to describe situations that result in stalled replication fork progression and the generation of extended regions of ssDNA (39). Replication stress can be induced by overexpression of oncogenes such as MYC family members or cyclin E, which can both deplete nucleotides as a result of deregulated origin firing and promote collisions between the transcription and replication machinery (40). Wee1 plays a key role in the replication stress response by regulating CDK2 and markers of replication stress such as pRPA have been shown to increase upon treatment with a Wee1 inhibitor (41). Immunoblot analysis revealed that CDX3, the model that is most sensitive to AZD1775, expressed high levels of L-Myc, cyclin E1, and phospho-RPA (**Fig. 6c**). Consistent with a recent report that tumors deficient for the histone methyltransferase SETD2 and ribonucleotide reductase subunit RRM2 are synthetic lethal with AZD1775 treatment (42), CDX3 expressed approximately half as much SETD2 and RRM2 compared to CDX4 and treatment with AZD1775 either alone or in combination with olaparib lead to modest reductions in RRM2 levels (**Supplementary Fig. 9a**, **b**) Moreover, AZD1775 treatment further increased pRPA levels in CDX3 but not CDX4 (**Fig. 6d**). Together these data suggest that both baseline and treatment-induced replication stress may predict sensitivity to AZD1775.

Discussion

SCLC is a cancer of high unmet need and, despite promising preclinical (43) and early clinical results (44) utilizing a DLL3-targeted antibody-drug conjugate, there have been no improvements in systemic therapy in three decades. Whilst approximately 100 SCLC trials have been registered on clinicaltrials.gov since 2007, strikingly few involved more than 100 patients, many are single arm studies, and correlative biomarker assessment is rarely obtained largely due to the difficulties in obtaining serial tumor biopsies. The statement in the US Recalcitrant Cancer Act 2012 that "more knowledge of the biology at different phases of SCLC is needed" can partially be attributed to the lack of relevant models. Indeed, the recently reported "patient-derived tumor encyclopedia" that contains over 1000 PDX does not contain a single SCLC model (45) and 21/26 SCLC PDX that have been published were derived prior to treatment of the donor patient with chemotherapy (43,46,47). Our CDX models and notably those obtained both at baseline and at progression after chemotherapy and reported here for the first time, offer a new approach to study acquired treatment resistance and test novel therapies in both first and second line settings. Utilizing these patient-relevant models derived from liquid biopsy, we demonstrated here that the combination of olaparib and AZD1775 exerted significant activity against a panel of SCLC CDX models that span the spectrum of responses to standard of care chemotherapy, with some demonstrating a profound and extended response to this novel combination.

The PARP inhibitor olaparib is currently being investigated in clinical trials, however the genetic determinants of drug sensitivity remain incompletely defined. Our CDX models offer the opportunity to investigate both predictive biomarkers and mechanisms of drug resistance. We observed the most striking combination efficacy in models where both monotherapies had some effect. Olaparib was most efficacious against CDX3, a model that failed to express homologous recombination repair protein PALB2. Although damaging *PALB2* mutations are reported to account for outlier responses to PARP inhibitors in other cancer types (48,49), targeted therapies that work in one cancer type do not necessarily work in another cancer type, even if the genetics are similar (e.g. vemurafenib in BRAF-mutant melanoma vs colorectal cancer (50)). To our knowledge this is the first report correlating a PALB2 mutation to combined olaparib/wee1 inhibition in SCLC. Moreover, SCLC tumors are not typically associated with defects in homologous recombination repair, a known predictive biomarker for PARP inhibitor sensitivity, and our data suggest further research into this area is warranted.

Multiple studies have shown that olaparib efficacy is significantly reduced against tumors pre-treated with chemotherapy. We sought to address this by examining the efficacy of olaparib/AZD1775 against a model generated from a patient who progressed on a platinum-based

therapy. Consistent with patient progression, CDX8p was resistant to treatment with platinum/etoposide. Although CDX8p was also relatively insensitive to olaparib/AZD1775, this combination elicited a more durable response than platinum/etoposide. Similarly, pre-treatment of CDX3 with platinum/etoposide blunted the response of chemonaive CDX3 to olaparib/AZD1775. Given the deep, though short lived response to patient standard of care platinum-based chemotherapy, it may be challenging to administer an olaparib/AZD1775 combination to treatment-naive SCLC patients. However, consideration should be given to minimising the number of chemotherapy cycles given to debulk the disease prior to testing this novel combination.

The exquisite sensitivity of CDX3 to combination therapy is likely due to the fact that both olaparib and AZD1775 exhibited single agent efficacy against this model. AZD1775 can both compromise the ability to restrain mitotic commitment in response to DNA damage and promote catastrophic DNA damage in G1/S via inappropriate activation of the MUS81-SLX4 nuclease (51). Thus, combinatorial activity of olaparib/AZD1775 may stem from AZD1775-induced inappropriate cleavage of stalled replication forks stemming from PARP trapping. However, our understanding of the biology of inappropriate induction of these pathways in S phase remains in its infancy and a detailed mechanistic understanding of what role PARP may play in this process remains beyond the scope of this study.

In addition to affecting sensitivity to olaparib, the *PALB2* mutation could potentially explain the response of CDX3 to AZD1775. BRCA2 and PALB2 function has been linked to replication fork stabilization/restart as part of the replication stress response. CDX3, the model that is most sensitive to AZD1775 single treatment, already has significantly elevated levels of replicative stress as indicated by elevated levels of L-Myc, cyclin E, and pRPA compared to the lesser responsive models. Moreover, we have demonstrated that following AZD1775 treatment there is a further increase in pRPA. Phosphorylated RPA can recruit PALB2 and BRCA2 to the stalled fork, and PALB2 loss has been associated with defects in the recovery of the stalled fork and therefore increased DNA damage (52). Additionally, BRCA2 and PALB2 are key regulators of the G2/M cell cycle checkpoint upon DNA damage (53). Therefore, the absence of PALB2 in combination with the inhibition of Wee1 could increase premature mitotic entry and therefore genomic instability in CDX3 cells. Together, these data suggest the efficacy of the olaparib/AZD1775 combination is likely to involve both an increase in replication stress response in S-phase as well as carryover of S-phase induced damage into mitosis.

Combination trials using PARP inhibitors are already in early phase development, including a second line study comparing temozolomide and veliparib with temozolomide and placebo where the

combination reported increased response rates but no significant difference in 4 month progression free survival (54). The ongoing Phase 1/2 trial of olaparib and temozolomide in patients progressing after chemotherapy also reported a 46% response rate for the combination compared to 14% for temozolomide alone (55). Olaparib/AZD1775 has demonstrated preclinical activity against AML(56), and a phase I clinical trial utilizing olaparib and AZD1775 has been initiated in patients with refractory solid tumors (https://ClinicalTrials.gov/show/NCT02511795), including SCLC, and an extended cohort in SCLC is planned.

Conversion of improved clinical response rates to lengthened progression free and overall survival will likely require development of robust predictive biomarkers. Our preclinical CDX data suggest that predicting the depth and duration of responses to olaparib and AZD1775 in SCLC patients is unlikely to be straightforward; the speed with which acquired chemotherapy resistance occurs, the genomic instability and heterogeneity of this devastating disease all point to the need for development of broad biomarker panels for the optimal use of this combination therapy, where different patients' tumors may acquire resistance via different and multiple molecular mechanisms. Further characterization of the DNA damage response status across a wide range of SCLC tumors, as well as functional validation of potential biomarkers is ongoing. Our results raise the possibility that a subset of SCLC may have defects in DNA damage response pathways that could be exploited by the combination of PARP and Wee1 inhibitors. Moreover, replication stress is often associated with oncogene overexpression and MYC family members, which are known to be amplified in approximately 20% SCLC and the role of MYC as a predictive biomarker of response to olaparib and AZD1775 can now be studied further in our burgeoning panel of 45 CDX models (57-59). The CDX3 cellular context represents a 'super responder' to the olaparib/AZD1775 combination and has revealed important molecular insights that we can now take forward in an assessment in the larger CDX panel.

Surgical specimens and archival biopsies are unlikely to reflect the disease after 1st or 2nd line treatments. We previously reported the prevalence of CTCs in SCLC (60), their prognostic significance and their potential as a readily obtained and repeatable source of pharmacodynamic and predictive biomarkers. Moreover, mutations in a panel of genes associated with DNA damage response measured in circulating tumor DNA may also assist patient selection. These liquid biopsy approaches should now be fully exploited in upcoming trials of novel therapies in SCLC where promising data in patient relevant preclinical models is forthcoming.

Acknowledgements

We would like to thank Matt Carter, Matt Lancashire, the CEP *in vivo* team, CRUK Manchester Institute core facilities, and the patients and their families. We thank Ian Hagan for his constructive comments on the manuscript. This research was supported by Cancer Research UK via core funding to the Cancer Research UK Manchester Institute (C5759/A27412), the Cancer Research UK Manchester Centre Award (C5759/A25254), the Cancer Research UK Lung Cancer Centre of Excellence Award (C5759/A20465), and the Cancer Research UK/AstraZeneca biomarkers alliance (10001080/AgrID486.

References

1. Bunn PA, Jr., Minna JD, Augustyn A, Gazdar AF, Ouadah Y, Krasnow MA*, et al.* Small Cell Lung Cancer: Can Recent Advances in Biology and Molecular Biology Be Translated into Improved Outcomes? J Thorac Oncol **2016**;11(4):453-74 doi 10.1016/j.jtho.2016.01.012.
2. Amarasena IU, Chatterjee S, Walters JA, Wood-Baker R, Fong KM. Platinum versus non-platinum chemotherapy regimens for small cell lung cancer. Cochrane Database Syst Rev **2015**(8):CD006849 doi 10.1002/14651858.CD006849.pub3.
3. Hodgkinson CL, Morrow CJ, Li Y, Metcalf RL, Rothwell DG, Trapani F*, et al.* Tumorigenicity and genetic profiling of circulating tumor cells in small-cell lung cancer. Nat Med **2014**;20(8):897-903 doi 10.1038/nm.3600.
4. Byers LA, Wang J, Nilsson MB, Fujimoto J, Saintigny P, Yordy J*, et al.* Proteomic profiling identifies dysregulated pathways in small cell lung cancer and novel therapeutic targets including PARP1. Cancer Discov **2012**;2(9):798-811 doi 10.1158/2159-8290.CD-12-0112.
5. Murai J, Huang SY, Das BB, Renaud A, Zhang Y, Doroshow JH*, et al.* Trapping of PARP1 and PARP2 by Clinical PARP Inhibitors. Cancer Res **2012**;72(21):5588-99 doi 10.1158/0008-5472.CAN-12-2753.
6. Strom CE, Johansson F, Uhlen M, Szigyarto CA, Erixon K, Helleday T. Poly (ADP-ribose) polymerase (PARP) is not involved in base excision repair but PARP inhibition traps a single-strand intermediate. Nucleic Acids Res **2011**;39(8):3166-75 doi 10.1093/nar/gkq1241.
7. Pommier Y, O'Connor MJ, de Bono J. Laying a trap to kill cancer cells: PARP inhibitors and their mechanisms of action. Sci Transl Med **2016**;8(362):362ps17 doi 10.1126/scitranslmed.aaf9246.
8. Lord CJ, Ashworth A. PARP inhibitors: Synthetic lethality in the clinic. Science **2017**;355(6330):1152-8 doi 10.1126/science.aam7344.
9. O'Connor MJ. Targeting the DNA Damage Response in Cancer. Mol Cell **2015**;60(4):547-60 doi 10.1016/j.molcel.2015.10.040.
10. Hirai H, Iwasawa Y, Okada M, Arai T, Nishibata T, Kobayashi M*, et al.* Small-molecule inhibition of Wee1 kinase by MK-1775 selectively sensitizes p53-deficient tumor cells to DNA-damaging agents. Mol Cancer Ther **2009**;8(11):2992-3000 doi 10.1158/1535-7163.MCT-09-0463.
11. Van Linden AA, Baturin D, Ford JB, Fosmire SP, Gardner L, Korch C*, et al.* Inhibition of Wee1 sensitizes cancer cells to antimetabolite chemotherapeutics in vitro and in vivo, independent of p53 functionality. Mol Cancer Ther **2013**;12(12):2675-84 doi 10.1158/1535-7163.MCT-13-0424.
12. Houghton PJ, Morton CL, Tucker C, Payne D, Favours E, Cole C*, et al.* The pediatric preclinical testing program: description of models and early testing results. Pediatr Blood Cancer **2007**;49(7):928-40 doi 10.1002/pbc.21078.
13. Carney DN, Bunn PA, Jr., Gazdar AF, Pagan JA, Minna JD. Selective growth in serum-free hormone-supplemented medium of tumor cells obtained by biopsy from patients with small cell carcinoma of the lung. Proc Natl Acad Sci U S A **1981**;78(5):3185-9.
14. Di Veroli GY, Fornari C, Wang D, Mollard S, Bramhall JL, Richards FM*, et al.* Combenefit: an interactive platform for the analysis and visualization of drug combinations. Bioinformatics **2016**;32(18):2866-8 doi 10.1093/bioinformatics/btw230.
15. Foucquier J, Guedj M. Analysis of drug combinations: current methodological landscape. Pharmacol Res Perspect **2015**;3(3):e00149 doi 10.1002/prp2.149.
16. He L, Kulesskiy E, Saarela J, Turunen L, Wennerberg K, Aittokallio T*, et al.* Methods for High-Throughput Drug Combination Screening and Synergy Scoring. Springer Protocols **2016**.
17. Khandelwal G, Girotti MR, Smowton C, Taylor S, Wirth C, Dynowski M*, et al.* Next-Gen Sequencing Analysis and Algorithms for PDX and CDX Models. Mol Cancer Res **2017** doi 10.1158/1541-7786.MCR-16-0431.

18. Fong PC, Yap TA, Boss DS, Carden CP, Mergui-Roelvink M, Gourley C*, et al.* Poly(ADP)-ribose polymerase inhibition: frequent durable responses in BRCA carrier ovarian cancer correlating with platinum-free interval. J Clin Oncol **2010**;28(15):2512-9 doi 10.1200/JCO.2009.26.9589.
19. van de Wetering M, Francies HE, Francis JM, Bounova G, Iorio F, Pronk A*, et al.* Prospective derivation of a living organoid biobank of colorectal cancer patients. Cell **2015**;161(4):933-45 doi 10.1016/j.cell.2015.03.053.
20. Yu M, Bardia A, Aceto N, Bersani F, Madden MW, Donaldson MC*, et al.* Cancer therapy. Ex vivo culture of circulating breast tumor cells for individualized testing of drug susceptibility. Science **2014**;345(6193):216-20 doi 10.1126/science.1253533.
21. Lallo A, Warpman Berglund U, Frese KK, Potter DS, Helleday T, Dive C. Ex vivo culture of circulating tumour cell derived explants to facilitate rapid therapy testing in small cell lung cancer. European Association for Cancer Research Annual Conference. Manchester, U.K.2016.
22. Dirix L, Swaisland H, Verheul HM, Rottey S, Leunen K, Jerusalem G*, et al.* Effect of Itraconazole and Rifampin on the Pharmacokinetics of Olaparib in Patients With Advanced Solid Tumors: Results of Two Phase I Open-label Studies. Clin Ther **2016**;38(10):2286-99 doi 10.1016/j.clinthera.2016.08.010.
23. Carrassa L, Chila R, Lupi M, Ricci F, Celenza C, Mazzoletti M*, et al.* Combined inhibition of Chk1 and Wee1: in vitro synergistic effect translates to tumor growth inhibition in vivo. Cell Cycle **2012**;11(13):2507-17 doi 10.4161/cc.20899.
24. Lord CJ, Ashworth A. BRCAness revisited. Nat Rev Cancer **2016**;16(2):110-20 doi 10.1038/nrc.2015.21.
25. Cardnell RJ, Feng Y, Diao L, Fan YH, Masrorpour F, Wang J*, et al.* Proteomic markers of DNA repair and PI3K pathway activation predict response to the PARP inhibitor BMN 673 in small cell lung cancer. Clin Cancer Res **2013**;19(22):6322-8 doi 10.1158/1078-0432.CCR-13-1975.
26. Du Y, Yamaguchi H, Wei Y, Hsu JL, Wang HL, Hsu YH*, et al.* Blocking c-Met-mediated PARP1 phosphorylation enhances anti-tumor effects of PARP inhibitors. Nat Med **2016**;22(2):194-201 doi 10.1038/nm.4032.
27. Liu X, Han EK, Anderson M, Shi Y, Semizarov D, Wang G*, et al.* Acquired resistance to combination treatment with temozolomide and ABT-888 is mediated by both base excision repair and homologous recombination DNA repair pathways. Mol Cancer Res **2009**;7(10):1686-92 doi 10.1158/1541-7786.MCR-09-0299.
28. Lok BH, Gardner EE, Schneeberger VE, Ni A, Desmeules P, Rekhtman N*, et al.* PARP Inhibitor Activity Correlates with SLFN11 Expression and Demonstrates Synergy with Temozolomide in Small Cell Lung Cancer. Clin Cancer Res **2017**;23(2):523-35 doi 10.1158/1078-0432.CCR-16-1040.
29. Murai J, Feng Y, Yu GK, Ru Y, Tang SW, Shen Y*, et al.* Resistance to PARP inhibitors by SLFN11 inactivation can be overcome by ATR inhibition. Oncotarget **2016**;7(47):76534-50 doi 10.18632/oncotarget.12266.
30. Stewart CA, Tong P, Cardnell RJ, Sen T, Li L, Gay CM*, et al.* Dynamic variations in epithelial-to-mesenchymal transition (EMT), ATM, and SLFN11 govern response to PARP inhibitors and cisplatin in small cell lung cancer. Oncotarget **2017** doi 10.18632/oncotarget.15338.
31. Konstantinopoulos PA, Ceccaldi R, Shapiro GI, D'Andrea AD. Homologous Recombination Deficiency: Exploiting the Fundamental Vulnerability of Ovarian Cancer. Cancer Discov **2015**;5(11):1137-54 doi 10.1158/2159-8290.CD-15-0714.
32. Mu Y, Lou J, Srivastava M, Zhao B, Feng XH, Liu T*, et al.* SLFN11 inhibits checkpoint maintenance and homologous recombination repair. EMBO Rep **2016**;17(1):94-109 doi 10.15252/embr.201540964.
33. Jaspers JE, Kersbergen A, Boon U, Sol W, van Deemter L, Zander SA*, et al.* Loss of 53BP1 causes PARP inhibitor resistance in Brca1-mutated mouse mammary tumors. Cancer Discov **2013**;3(1):68-81 doi 10.1158/2159-8290.CD-12-0049.

34. Xu G, Chapman JR, Brandsma I, Yuan J, Mistrik M, Bouwman P*, et al.* REV7 counteracts DNA double-strand break resection and affects PARP inhibition. Nature **2015**;521(7553):541-4 doi 10.1038/nature14328.
35. Matheson CJ, Backos DS, Reigan P. Targeting WEE1 Kinase in Cancer. Trends Pharmacol Sci **2016**;37(10):872-81 doi 10.1016/j.tips.2016.06.006.
36. Clausse V, Goloudina AR, Uyanik B, Kochetkova EY, Richaud S, Fedorova OA*, et al.* Wee1 inhibition potentiates Wip1-dependent p53-negative tumor cell death during chemotherapy. Cell Death Dis **2016**;7:e2195 doi 10.1038/cddis.2016.96.
37. Toledo CM, Ding Y, Hoellerbauer P, Davis RJ, Basom R, Girard EJ*, et al.* Genome-wide CRISPR-Cas9 Screens Reveal Loss of Redundancy between PKMYT1 and WEE1 in Glioblastoma Stem-like Cells. Cell Rep **2015**;13(11):2425-39 doi 10.1016/j.celrep.2015.11.021.
38. Dobbelstein M, Sorensen CS. Exploiting replicative stress to treat cancer. Nat Rev Drug Discov **2015**;14(6):405-23 doi 10.1038/nrd4553.
39. Forment JV, O'Connor MJ. Targeting the replication stress response in cancer. Pharmacol Ther **2018** doi 10.1016/j.pharmthera.2018.03.005.
40. Garcia-Muse T, Aguilera A. Transcription-replication conflicts: how they occur and how they are resolved. Nat Rev Mol Cell Biol **2016**;17(9):553-63 doi 10.1038/nrm.2016.88.
41. Saini P, Li Y, Dobbelstein M. Wee1 is required to sustain ATR/Chk1 signaling upon replicative stress. Oncotarget **2015**;6(15):13072-87 doi 10.18632/oncotarget.3865.
42. Pfister SX, Markkanen E, Jiang Y, Sarkar S, Woodcock M, Orlando G*, et al.* Inhibiting WEE1 Selectively Kills Histone H3K36me3-Deficient Cancers by dNTP Starvation. Cancer Cell **2015**;28(5):557-68 doi 10.1016/j.ccell.2015.09.015.
43. Saunders LR, Bankovich AJ, Anderson WC, Aujay MA, Bheddah S, Black K*, et al.* A DLL3-targeted antibody-drug conjugate eradicates high-grade pulmonary neuroendocrine tumor-initiating cells in vivo. Sci Transl Med **2015**;7(302):302ra136 doi 10.1126/scitranslmed.aac9459.
44. Hamilton EP, Wang JS, Falchook G, Fields-Jones S, Cook C, Mugundu G*, et al.* A phase Ib study of AZD1775 and olaparib combination in patients with refractory solid tumors. Journal of Clinical Oncology **2016**;34(15_suppl):5562- doi 10.1200/JCO.2016.34.15_suppl.5562.
45. Gao H, Korn JM, Ferretti S, Monahan JE, Wang Y, Singh M*, et al.* High-throughput screening using patient-derived tumor xenografts to predict clinical trial drug response. Nat Med **2015**;21(11):1318-25 doi 10.1038/nm.3954.
46. Gardner EE, Lok BH, Schneeberger VE, Desmeules P, Miles LA, Arnold PK*, et al.* Chemosensitive Relapse in Small Cell Lung Cancer Proceeds through an EZH2-SLFN11 Axis. Cancer Cell **2017**;31(2):286-99 doi 10.1016/j.ccell.2017.01.006.
47. Nemati F, Bras-Goncalves R, Fontaine JJ, de Pinieux G, De Cremoux P, Chapelier A*, et al.* Preclinical assessment of cisplatin-based therapy versus docetaxel-based therapy on a panel of human non-small-cell lung cancer xenografts. Anticancer Drugs **2009**;20(10):932-40 doi 10.1097/CAD.0b013e32833009cc.
48. Buisson R, Dion-Cote AM, Coulombe Y, Launay H, Cai H, Stasiak AZ*, et al.* Cooperation of breast cancer proteins PALB2 and piccolo BRCA2 in stimulating homologous recombination. Nat Struct Mol Biol **2010**;17(10):1247-54 doi 10.1038/nsmb.1915.
49. Smith MA, Hampton OA, Reynolds CP, Kang MH, Maris JM, Gorlick R*, et al.* Initial testing (stage 1) of the PARP inhibitor BMN 673 by the pediatric preclinical testing program: PALB2 mutation predicts exceptional in vivo response to BMN 673. Pediatr Blood Cancer **2015**;62(1):91-8 doi 10.1002/pbc.25201.
50. Kopetz S, Desai J, Chan E, Hecht JR, O'Dwyer PJ, Maru D*, et al.* Phase II Pilot Study of Vemurafenib in Patients With Metastatic BRAF-Mutated Colorectal Cancer. J Clin Oncol **2015**;33(34):4032-8 doi 10.1200/JCO.2015.63.2497.

51. Duda H, Arter M, Gloggnitzer J, Teloni F, Wild P, Blanco MG*, et al.* A Mechanism for Controlled Breakage of Under-replicated Chromosomes during Mitosis. Dev Cell **2017**;40(4):421-2 doi 10.1016/j.devcel.2017.02.015.
52. Murphy AK, Fitzgerald M, Ro T, Kim JH, Rabinowitsch AI, Chowdhury D*, et al.* Phosphorylated RPA recruits PALB2 to stalled DNA replication forks to facilitate fork recovery. J Cell Biol **2014**;206(4):493-507 doi 10.1083/jcb.201404111.
53. Menzel T, Nahse-Kumpf V, Kousholt AN, Klein DK, Lund-Andersen C, Lees M*, et al.* A genetic screen identifies BRCA2 and PALB2 as key regulators of G2 checkpoint maintenance. EMBO Rep **2011**;12(7):705-12 doi 10.1038/embor.2011.99.
54. Pietanza MC, Krug LM, Waqar SN, Dowlati A, Hann CL, Chiappori A*, et al.* A multi-center, randomized, double-blind phase II study comparing temozolomide (TMZ) plus either veliparib (ABT-888), a PARP inhibitor, or placebo as 2nd or 3rd-line therapy for patients (Pts) with relapsed small cell lung cancers (SCLCs). J Clin Oncol **2016**;34(suppl; abstr 8512).
55. Farago AF, Drapkin BJ, Charles A, Yeap B, Heist RS, Azzoli CG*, et al.* CT048 - Phase 1/2 study of olaparib tablets and temozolomide in patients with small cell lung cancer (SCLC) following failure of prior chemotherapy. 2017; Washignton D.C.
56. Garcia TB, Snedeker JC, Baturin D, Gardner L, Fosmire SP, Zhou C*, et al.* A Small-Molecule Inhibitor of WEE1, AZD1775, Synergizes with Olaparib by Impairing Homologous Recombination and Enhancing DNA Damage and Apoptosis in Acute Leukemia. Mol Cancer Ther **2017**;16(10):2058-68 doi 10.1158/1535-7163.MCT-16-0660.
57. Iwakawa R, Kohno T, Totoki Y, Shibata T, Tsuchihara K, Mimaki S*, et al.* Expression and clinical significance of genes frequently mutated in small cell lung cancers defined by whole exome/RNA sequencing. Carcinogenesis **2015**;36(6):616-21 doi 10.1093/carcin/bgv026.
58. Peifer M, Fernandez-Cuesta L, Sos ML, George J, Seidel D, Kasper LH*, et al.* Integrative genome analyses identify key somatic driver mutations of small-cell lung cancer. Nat Genet **2012**;44(10):1104-10 doi 10.1038/ng.2396.
59. Sos ML, Dietlein F, Peifer M, Schottle J, Balke-Want H, Muller C*, et al.* A framework for identification of actionable cancer genome dependencies in small cell lung cancer. Proc Natl Acad Sci U S A **2012**;109(42):17034-9 doi 10.1073/pnas.1207310109.
60. Hou JM, Krebs MG, Lancashire L, Sloane R, Backen A, Swain RK*, et al.* Clinical significance and molecular characteristics of circulating tumor cells and circulating tumor microemboli in patients with small-cell lung cancer. J Clin Oncol **2012**;30(5):525-32 doi 10.1200/JCO.2010.33.3716.

Table 1

Model	Pt treatment	Tumor response[1]	Chemosensitivity	Pt survival (days)[1]	CellSearch count[2]
2	carbo/etop	PR	refractory	108	1625
3	carbo/etop	PR	sensitive	295	507
3p		relapse		295	463
4	carboplatin	PD	refractory	27	1375
8	carboplatin	PR	refractory	181	388
8p		relapse		181	1796
10	carbo/etop	PR	sensitive	317	160
14p		relapse		227	362
15p		relapse		556	361
15p2		relapse		556	165

[1] Survival is defined as the time from diagnosis until death
[2] The number of EpCAM+/CK+ CTC's in a parallel 7.5ml blood sample taken from the same patient bleed that yielded the corresponding CDX.

Figure Legends

Figure 1. Combination treatment with olaparib/AZD1775 is superior to cisplatin/etoposide. **a**) The cohort average best response (+/- sd) is shown for cisplatin/etoposide (white), AZD1775 (red), olaparib (green), or the AZD1775/olaparib (blue). **b**) The cohort average benefit (+/- sd) of each treatment over vehicle is shown for each treatment. Cohort sizes are $\geq$ 7. * p<0.05; ** p<0.005 vs. cisplatin/etoposide treatment.

Figure 2. AZD1775 and olaparib are synergistic *in vitro*. CDX3 (**a**), CDX4 (**b**), CDX8 (**c**), or CDX8p (**d**) *ex vivo* cultures were treated with AZD1775 and olaparib for 1 week and relative cell viability was assessed. One representative experiment of at least three is shown. For the combinatorial index, red is indicative of synergy and green is indicative of antagonism between drugs. **e)** GI_{50} values for various CDX *ex vivo* cultures treated with cisplatin, etoposide, AZD1775, or olaparib are shown after 1 week of drug treatment. For the combination we have shown the GI_{50} values for olaparib at 150 nM AZD1775.

Figure 3. Pharmacokinetic analyses. **a**) Mice were treated with 100 mg kg^{-1} (dark green) or 50 mg kg^{-1} (dashed green) olaparib, or with a combination of low dose olaparib and AZD1775 (blue) for 21 days and tumor volumes were measured biweekly. Individual relative tumor volumes are depicted. Tumor lysates from cohorts of mice bearing different CDX models treated with AZD1775 (red), olaparib (green), or the combination (blue) were analysed and quantified for AZD1775 (**b**) or olaparib (**c**) at 2 hours after a single dose. Dashed lines represent the reliable limits of detection. Cohorts of $\geq$ 4 tumors were used.

Figure 4. Pharmacodynamic analyses. Tumor lysates from cohorts of mice bearing different CDX models treated with a single dose of vehicle (white), AZD1775 (red), olaparib (green), or the combination (blue) were analysed and quantified. Cohorts of $\geq$ 4 tumors were used. **a**) pCDK1 levels were measured by immunoblotting 2 hours after a single dose and normalised to both total CDK1 and vinculin in each sample. **b**) Total PAR levels were measured by ELISA 2 hours after a single dose. The dashed line indicates the limit of detection (2pg/ml). Proof of concept and proof of mechanism biomarkers were measured by quantitative immunohistochemistry for pHH3 at 2 hours (**c**), CC3 at 24 hours (**d**), pCHK1 at 2 hours (**e**), and γH2AX at 24 hours (**f**) after dosing. * p<0.05, **p<0.005

Figure 5. Deficient double strand break repair in CDX3. **a**) CDX3, CDX4, CDX8, and CDX8p *ex vivo* cultures were irradiated at indicated doses in triplicate and relative cell viability was assessed 5 days later. One of three representative experiments is shown. **b**) At indicated times following irradiation,

CDX3 and CDX4 cultures were assessed for Rad51 focus formation. Geminin and DAPI staining was used to identify cells in G2, and these results were quantified by a semi-automated computer algorithm. The dashed line indicates a threshold above which cells are considered positive for damage-induced focus formation. **p<0.005 **c**) Sanger sequencing identified the E178* *PALB2* mutation in CDX3, but not CDX4. **d**) Schematic of PALB2 with protein-protein interaction domains shown in grey and the E178* mutation shown in red.

Figure 6. Sensitivity to AZD1775 correlates with markers of replication stress. **a**) Immunoblot analysis of duplicate tumor lysates for indicated proteins. The p53 mutation associated with a given model is indicated. The positive control for RB is the H1694 cell line. **b**) Representative images and quantification of $p21^{CIP1}$ IHC from CDX3, CDX4, CDX8, and CDX8p. $p21^{CIP1}$ levels are plotted against tumor regression values for each model. **c**) Immunoblot analysis of duplicate tumor lysates for indicated proteins. Corresponding average RPKM values for L-Myc and C-Myc in each model are indicated below immunoblots. N-Myc expression was not investigated, however RPKM values below 5 suggest it is not expressed in the models investigated. **d**) Immunoblot analysis of duplicate lysates from CDX3 and CDX4 tumors treated with vehicle or AZD1775 for 24 hours. The positive control for L-Myc is the H1694 cell line.

Figure 1

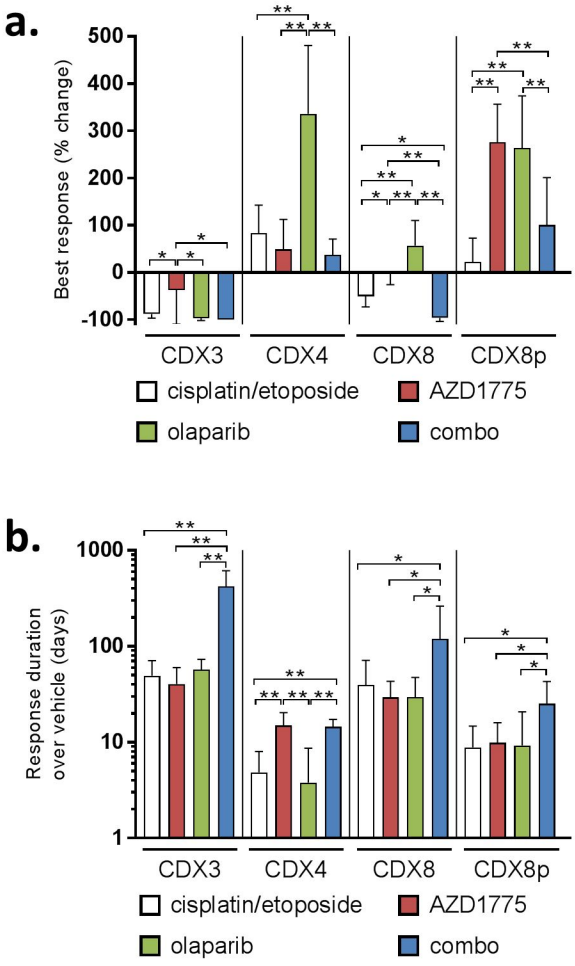

Figure 2

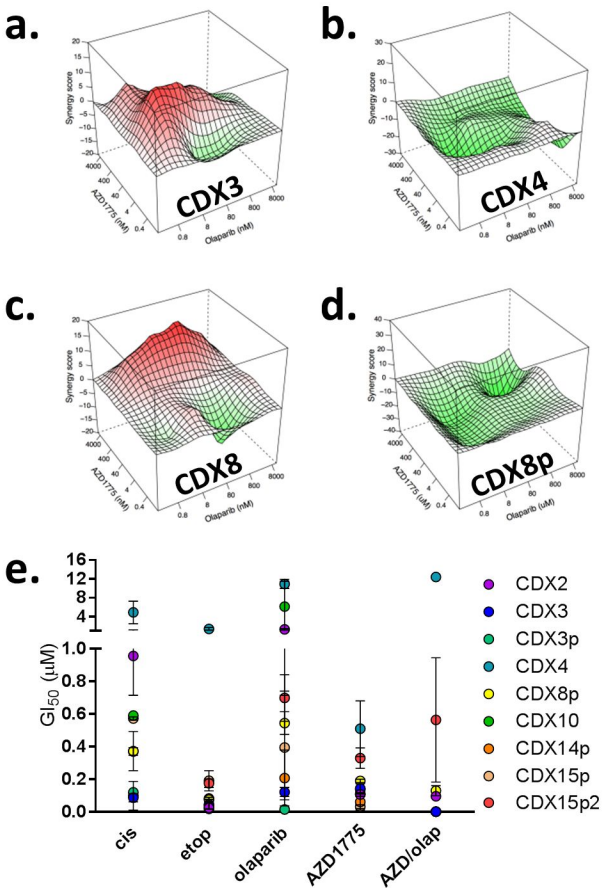

Figure 3

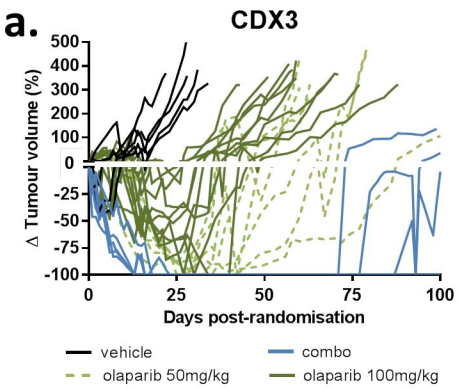

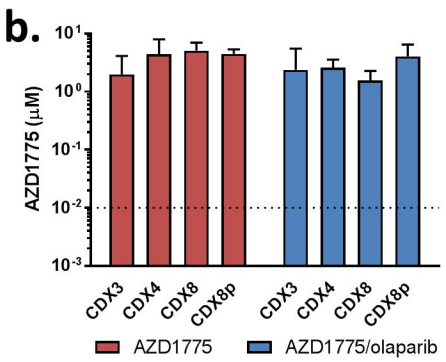

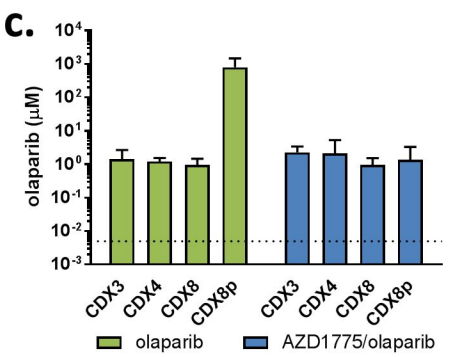

Figure 4

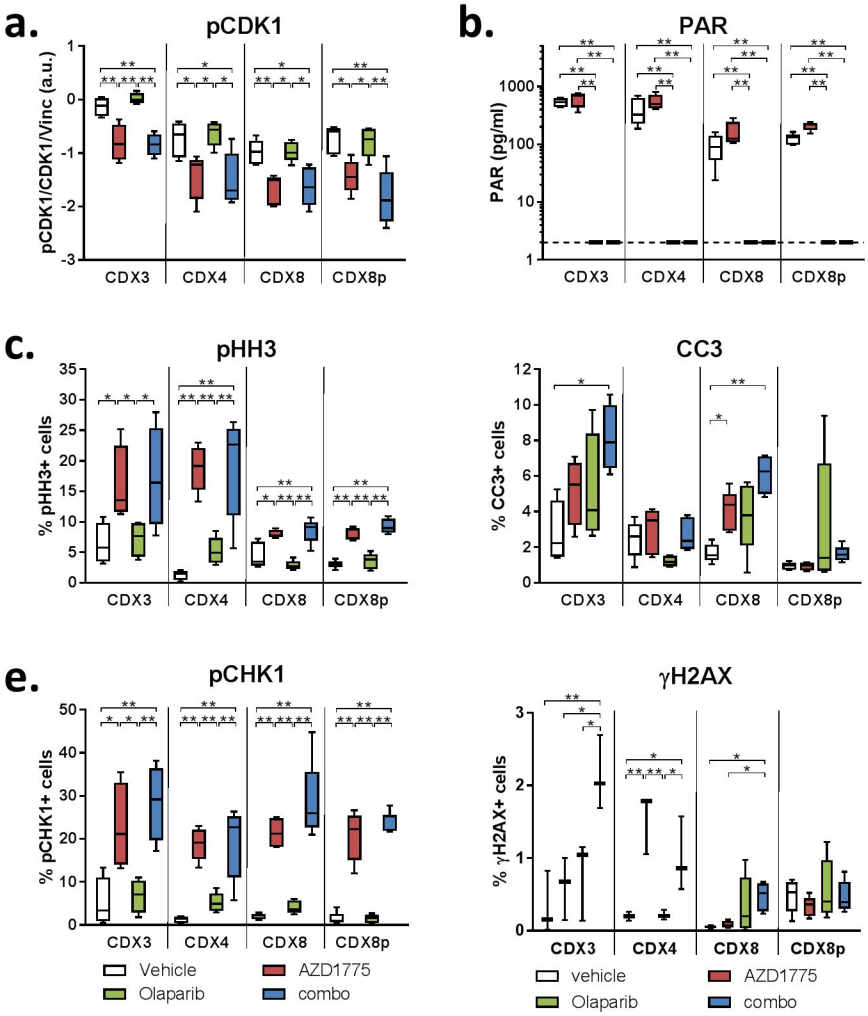

Figure 5

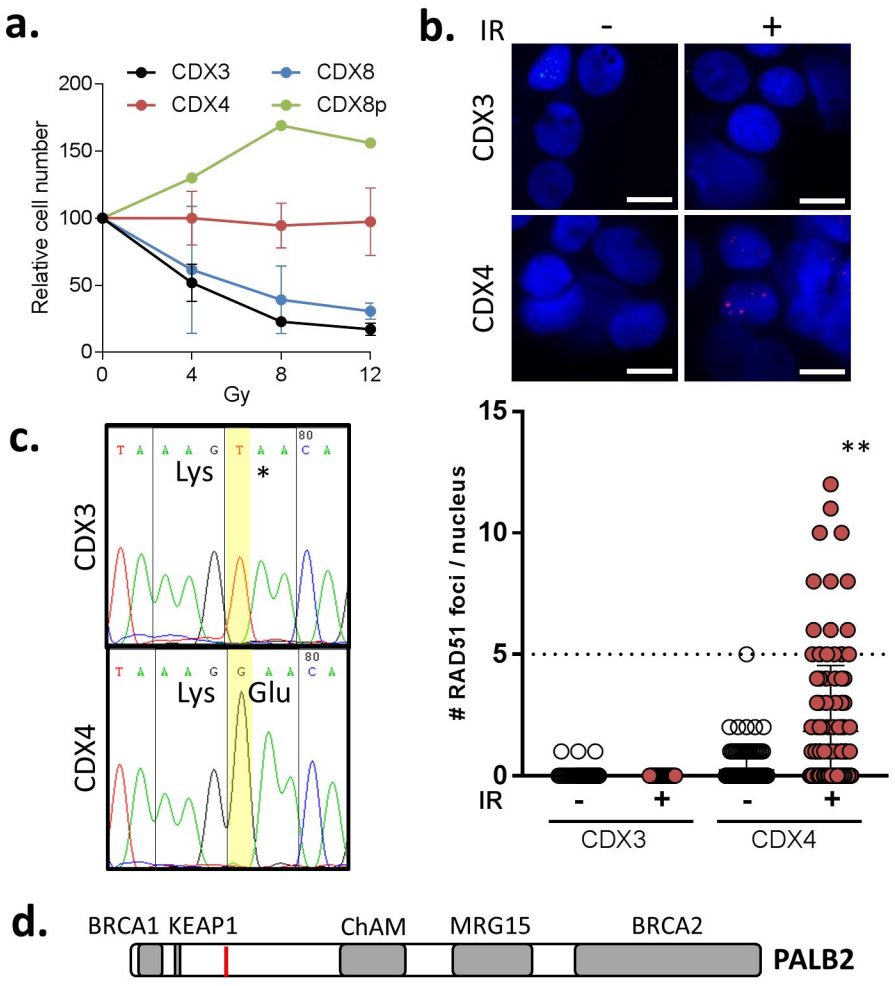

Figure 6

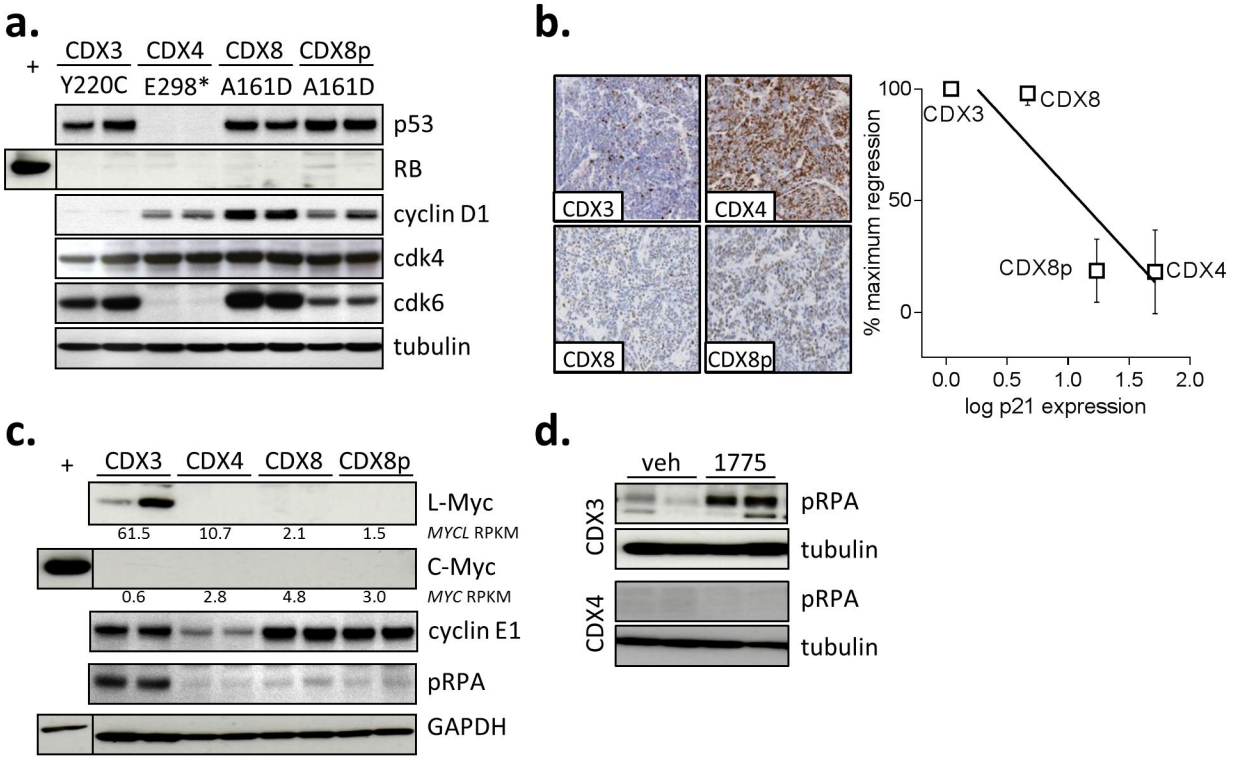

AACR American Association for Cancer Research

Clinical Cancer Research

The combination of the PARP inhibitor olaparib and the Wee1 inhibitor AZD1775 as a new therapeutic option for small cell lung cancer

Alice Lallo, Kristopher K Frese, Christopher Morrow, et al.

Clin Cancer Res Published OnlineFirst June 25, 2018.